

## THE ORIGIN OF B-TYPE RUNAWAY STARS: NON-LTE ABUNDANCES AS A DIAGNOSTIC

CATHERINE M. MCEVOY<sup>1,2,3</sup>, PHILIP L. DUFTON<sup>1</sup>, JONATHAN V. SMOKER<sup>2,1</sup>, DAVID L. LAMBERT<sup>4</sup>, FRANCIS P. KEENAN<sup>1</sup>, FABIAN R. N. SCHNEIDER<sup>5</sup>,  
WILLEM-JAN DE WIT<sup>2</sup>

*Draft version April 25, 2022*

### ABSTRACT

There are two accepted mechanisms to explain the origin of runaway OB-type stars: the Binary Supernova Scenario (BSS), and the Cluster Ejection Scenario (CES). In the former, a supernova explosion within a close binary ejects the secondary star, while in the latter close multi-body interactions in a dense cluster cause one or more of the stars to be ejected from the region at high velocity. Both mechanisms have the potential to affect the surface composition of the runaway star. TLUSTY non-LTE model atmosphere calculations have been used to determine atmospheric parameters and carbon, nitrogen, magnesium and silicon abundances for a sample of B-type runaways. These same analytical tools were used by Hunter et al. (2009) for their analysis of 50 B-type open cluster Galactic stars (i.e. non-runaways). Effective temperatures were deduced using the silicon-ionization balance technique, surface gravities from Balmer line profiles and microturbulent velocities derived using the Si spectrum. The runaways show no obvious abundance anomalies when compared with stars in the open clusters. The runaways do show a spread in composition which almost certainly reflects the Galactic abundance gradient and a range in the birthplaces of the runaways in the Galactic disk. Since the observed Galactic abundance gradients of C, N, Mg and Si are of a similar magnitude, the abundance ratios (e.g., N/Mg) are, as obtained, essentially uniform across the sample.

*Subject headings:* stars: early-type – stars: atmospheres – stars: runaways – stars: rotation

### 1. INTRODUCTION

The presence of a significant number of early-type OB main sequence stars in the Galactic halo, as demonstrated by Greenstein & Sargent (1974), has occasioned an extensive literature on the origins of massive young stars far from the Galactic disk, the richest site of star-forming regions. Very broadly, two explanations for halo OB main sequence stars have survived scrutiny; both explanations consider that the stars formed in the Galactic disk and were ejected from their parental open cluster or association with sufficient velocity to reach the Galactic halo. Then, the stars deserve their common classification as ‘runaway’ stars. A less likely explanation not considered further here is that the halo OB main sequence stars were formed *in situ* (Dyson & Hartquist 1983).

Two proposed scenarios are considered capable of producing runaway stars: the binary supernova scenario (here, BSS) and the cluster ejection scenario (here, CES):

- In the BSS proposed first by Zwicky (1957) and developed by Blaauw (1961), the runaway star was the secondary in a binary with a more massive star which experienced its terminal supernova explosion. The reduced gravitational attraction of the primary’s stellar remnant, either a neutron star or a black hole, freed the secondary to escape with a velocity similar to its orbital velocity. The escaping secondary - the runaway star - may be accompanied by the stellar remnant.
- In the CES proposed by Poveda et al. (1967), close encoun-

ters in a young open cluster may lead to ejection of a star. Multi-body interactions are favored to eject a single or a binary star. Simulations suggest that the most effective way to produce high-velocity runaway stars is through the interaction of two hard binary systems (Hoffer 1983). Leonard (1989) and Leonard & Fahlman (1991) show that binary-binary interactions may result in runaway single, binary or even merged binary stars.

As might be expected, both BSS and CES contribute to the runaway population. Hoogerwerf et al. (2001 - see also de Zeeuw et al. 2001) use astrometric data to predict past tracks of stars in the Galaxy to show that specific examples of runaways may be attributed to the BSS (see  $\zeta$  Oph and pulsar PSR J1392+1059) or to the CES (AE Aur and  $\mu$  Col ejected from Orion – see Blaauw & Morgan (1954) and Gies & Bolton (1986). Across their sample of runaways, Hoogerwerf et al. estimate that two-thirds arise from the BSS and one-third from the CES. Other authors consider the CES the greater contributor of runaway stars.

In this paper, we provide a non-LTE analysis of C, N, Mg and Si abundances for a sample of runaway B stars and search for abundance differences among the sample and between the sample and B stars in young open clusters in the Galactic disk. The goal is to determine, if the abundance information provides convincing evidence or even intriguing clues to the origin of a runaway. The suggestion to exploit chemical composition to judge competing origins of runaway stars is traceable to Blaauw (1993) who suggested a study of the He/H abundance versus projected rotational velocity  $v \sin i$  with He enrichment and high  $v \sin i$  resulting from the BSS. Helium enrichment should generally be accompanied by N enrichment and a parallel C deficiency as a result of H-burning by the CNO-cycles. A Mg and Si enrichment of the runaway star might result for stars provided by the BSS but not the CES. Many previous studies have reported LTE abundance analy-

<sup>1</sup> Astrophysics Research Centre, School of Mathematics and Physics, Queen’s University Belfast, Belfast BT7 1NN, UK

<sup>2</sup> European Southern Observatory, Alonso de Cordova 3107, Casilla 19001, Vitacura, Santiago 19, Chile

<sup>3</sup> Graduate School, King’s College London, London SE1 9NH, UK

<sup>4</sup> The University of Texas at Austin, Department of Astronomy, RLM 16,316, Austin, TX 78712

<sup>5</sup> Department of Physics, University of Oxford, Denys Wilkinson Building, Keble Road, Oxford OX1 3RH, UK

ses generally giving abundances relative to Galactic disk B stars of the same atmospheric parameters - see, for example, the runaway sample analyzed by Martin (2004). This is the first non-LTE analysis of a sample of runaway B stars.

In Section 2, we discuss selection criteria used to isolate our sample of runaway stars whose spectra were obtained (see Section 3) and analyzed in Section 4 following the method previously applied by Hunter et al. (2009 - see also Trundle et al. 2007) to B stars in the three Galactic open clusters. Abundances in the runaway and cluster B stars are discussed in Section 5. Rotational and radial velocities are discussed in Section 6. Brief concluding remarks are offered in Section 7.

## 2. SELECTION OF RUNAWAY B STARS

Targets were selected from catalogues of previously identified runaway candidates. Different criteria are outlined in each source identified in the reference column of Table 1 and cited in the footnotes. All objects in our sample either lie far from the Galactic plane with a height above or below the plane ( $z$  distance) of  $> 0.3$  kpc or have high Galactic latitude ( $|b| > 30^\circ$ ) or a peculiar space velocity of  $\gtrsim 30 \text{ km s}^{-1}$ . A star that meets any one of these criteria is considered a runaway. Essentially each star in our sample has been shown by one or more of the references to have been ejected from the disk, i.e., the travel time from disk to its halo location is less than the lifetime of the star. In the BSS it is expected that the ejection velocity gained from the loss of mass from the binary system as a result of the supernova will not exceed  $300\text{-}400 \text{ km s}^{-1}$ , while for CES, similar velocities are possible (see Leonard 1993; Portegies Zwart 2000; Gvaramadze et al. 2009). A majority of the runaway stars are expected to be bound to the Galaxy. Stars exceeding the escape velocity are generally called ‘hypervelocity’ stars and, the principal ejection engine for such stars is the Galaxy’s central supermassive blackhole (see review by Brown 2015). Two hypervelocity stars originating in the outer Galaxy are known: HD 271791 (Heber et al. 2008; Przybilla et al. 2008) and HIP 60350 (Irrgang et al. 2010). Such stars may be products of the BSS operating in a binary having particular initial masses.

One of our two primary sources of runaway B stars is a list by Silva & Napiwotzki (2011) of 174 high Galactic latitude B stars drawn from the literature. As noted by Silva & Napiwotzki and emphasized by essentially all previous discussion of runaway B stars, spectral classification of B-type does not ensure that the star is a B main sequence (massive) star because low mass stars evolving either off the blue horizontal branch or from the asymptotic branch stars (i.e., post-AGB stars) can encroach on the effective temperature - surface gravity plane ( $T_{\text{eff}}, \log g$ ) plane occupied by main sequence B stars - see also Tobin (1987). Using then available information on ( $T_{\text{eff}}, \log g$ ) and data on atmospheric abundances, Silva & Napiwotzki identified which of the 174 stars belong or possibly belong to the main sequence (MS or MS?). With one exception, the stars we observed from Silva & Napiwotzki’s Tables 2 and 3 were classified as MS or MS?. The one exception is HIP 60615 (BD +36 2268) which was classified Non-MS. As massive stars, the combination of effective temperature and surface gravity indicate that the sample spans the mass range of about 5–25 solar masses. Estimated ejection velocities range up to about  $400 \text{ km s}^{-1}$  (Silva & Napiwotzki 2011) and do not lead to escape from the Galaxy. Actual space velocities of observed runaways are smaller than the ejection velocities because stars are generally observed near the apex

of their orbit where they spend most of their time.

Our second primary source of runaway B stars is the catalogue of young runaway stars within 3 kpc of the Sun compiled by Tetzlaff et al. (2011) using *Hipparcos* astrometry. From this catalogue of more than 2500 stars younger than about 50 My and with peculiar velocities, we selected 13 B stars and of these six belong also to our selection from Silva & Napiwotzki.

Our sample was completed by selecting another 10 targets from the literature on runaway stars.

References to all sources providing runaway stars are noted in Table 1 listing 38 stars. The table lists the stars by their HIP number where available and/or an alternative designation, the  $V$  magnitude, the spectral type, the source of our spectra (see next Section), the radial velocity ( $v_r$ ), the projected rotational velocity ( $v \sin i$ ) and the reference to the star’s selection as a runaway B star.

## 3. OBSERVATIONS

High-resolution high signal-to-noise optical spectra were collected from three telescopes over a period of 16 months. Wavelength coverage and observation dates of each dataset are shown in Table 2. Each set of observations is described below, along with the reduction procedures through which they were prepared for analysis.

### 3.1. FEROS Observations

Twenty six targets were observed in August 2014, using the ESO - FEROS instrument (Kaufer et al. 1999), a high resolution ( $R \approx 48,000$ ) prism cross-dispersed echelle spectrograph. FEROS has almost complete spectral coverage from  $3500\text{--}9200 \text{ \AA}$  and provides high SNR ( $\approx 300$  - see Table 2) in relatively short exposure times for bright stars. All data were reduced using the ESO FEROS pipeline (version 1.57). Multiple exposures were combined using either a median or weighted average, within IRAF<sup>6</sup>. Both these methods of merging the exposures resulted in very similar spectra, with the weighted average giving a slightly higher signal-to-noise ratio, and so these were adopted. Occasionally cosmic ray events were visible, but these were easily removed from the spectra manually, if they interfered with any analysis.

Four targets (HD 1999, HD 165955, HD 204076 and HD 208213) were deemed unusable for abundance analysis. HD 1999 showed double lines in its spectrum, making quantitative analysis unreliable. HD 165955 has a very high  $v \sin i$  and so many lines became unobservable. HD 204076 proved to be double-lined spectroscopic binary when observed with UVES. HD 208213 did not have a sufficient SNR to identify Si III lines required for our analysis. It was also observed with UVES and discarded for the same reason.

### 3.2. UVES Observations

Seventeen targets were observed at the VLT using the UVES instrument (Dekker et al. 2000), a high resolution ( $R \approx 80,000$ ), high efficiency, cross-dispersed echelle spectrograph with a blue and a red arm. A standard setting (437 + 760) was used, yielding a wavelength coverage of  $3730\text{--}4990 \text{ \AA}$  in the blue arm and  $5650\text{--}9460 \text{ \AA}$  in the red. All of the data

<sup>6</sup> IRAF is distributed by the National Optical Astronomy Observatory, which is operated by the Association of Universities for Research in Astronomy (auRA) under cooperative agreement with the National Science Foundation.

TABLE 1

EACH STAR LISTED BY HIP NUMBER, ALONG WITH AN ALTERNATIVE IDENTIFIER. V MAGNITUDES, SPECTRAL TYPES, INSTRUMENT USED FOR OBSERVATION, RADIAL VELOCITY, PROJECTED ROTATIONAL VELOCITY AND THE REFERENCE THAT IDENTIFIES THE STAR AS A RUNAWAY.

HIP	Other	Vmag	Spec. type	Obs. <sup>a</sup>	$v_r$ km-s <sup>-1</sup>	$v \sin i$ km-s <sup>-1</sup>	Ref <sup>b</sup>
2702	HD 3175	9.33	B4V	F	-13±2	26±2	S11
3812	CD -56 152	10.18	B2V	U	14±8	194±7	S11
7873	HD 10747	8.15	B2V	F	-9±2	15±1	T11
13489	HD 18100	8.44	B5II/III	F	80±7	241±6	M05
16758	HD 22586	9.33	B4V	F	-13±2	88±3	S11
45563	HD 78584	8.20	B3	T	-120±6	102±4	T11
55051	HD 97991	7.41	B2/3V	U	31±3	135±3	S11
56322	HD 100340	10.12	B0	T,U	253±10	181±10	S11
60615	BD +36 2268	10.31	B3V	T	31±4	54±4	S11
61431	HD 109399	7.67	B0.5III	F	-43±3	203±6	T11
64458	HD 114569	8.10	B7/8	F	104±2	74±1	M12
67060	HD 119608	7.53	B1Ib	F	31±1	59±9	M04
68297	HD 121968	10.26	B1V	T,U	17±9	199±27	S11
70205	LP 857-24	11.36	...	F	243±4	64±4	B12
70275	HD 125924	9.66	B2IV	T	244±1	64±3	S11
79649	HD 146813	9.06	B1.5	T	21±2	87±3	S11
81153	HD 149363	7.81	B0.5III	F,T,U	145±3	88±10	S11
85729	HD 158243	8.15	B1Ib	F	-63±2	70±2	M12
91049	HD 171871	7.78	B2IIp	T	-64±1	44±1	T11
92152	HD 173502	9.70	B1II	F	49±1	53±3	K82
94407	HD 179407	9.44	B0.5Ib	F	-120±4	134±9	S97
96130	HD 183899	9.93	B2III	F	-46±2	55±3	S11, T11
98136	HD 188618	9.38	B2II	F	46±4	167±3	S11
101328	HD 195455	9.20	B0.5III	F,U	19±7	213±7	S11
105912	HD 204076	8.73	B1V	F,U	0±3	102±1	S11, T11
107027	HD 206144	9.34	B2II	F,U	122±5	184±12	S11
109051	HD 209684	9.94	B2/3III	U	82±2	108±3	S11, T11
111563	HD 214080	6.93	B1/2Ib	F	16±2	108±3	S11
112022	HD 214930	7.40	B2IV	T	-60±4	12±1	M05
112482	HD 215733	7.34	B1II	T	-6±6	72±1	T11
113735	HD 217505	9.13	B2III/IV	F	-17±1	26±2	S11
114690	HD 219188	7.06	B0.5III	F,T	73±19	239±15	S11
115347	HD 220172	7.64	B3Vn	F	26±2	39±1	S11
115729	HD 220787	8.29	B3III	F	26±2	26±2	S11, T11
...	EC 05582-5816	9.46	B3V	F	85±13	221±5	S11
...	EC 13139-1851	10.50	B4	U	15±4	43±1	S11
...	EC 20140-6935	8.83	B2V	F	-24±2	45±2	S11
...	PB 5418	11.35	B2	U	147±3	50±1	S11
...	PHL 159	10.90	B	U	87±2	30±1	S11

Note: <sup>a</sup> Spectrograph used for the observation: F=Feros, T=Tull and U=UVES

<sup>b</sup> References: S11=Silva & Napiwotzki (2011), T11=Tetzlaff et al. (2011), M05=Mdzinarishvili & Chargeishvili (2005), M12=McDonald et al. (2012), M04=Martin (2004), B12= de Bruijne & Eilers (2012), K82=Keenan et al. (1982), S97=Smartt et al. (1997).

TABLE 2

OBSERVATION DATES AND WAVELENGTH COVERAGE OF EACH INSTRUMENT

Instrument	$\lambda$ coverage (Å)	Dates
FEROS	3500 – 9200	August 2013
Tull	3400 – 10900	May/June 2013
UVES blue arm	3730 – 4990	March-July 2014
UVES red arm	5650 – 9460	March-July 2014

were taken directly from the ESO archive, having been reduced using the ESO UVES pipeline (Ballester et al. 2000). Multiple exposures were normalised and combined using either a median or weighted  $\sigma$ -clipping algorithm, within IDL. As the SNR of the individual exposures was high, the final spectra from both methods were effectively indistinguishable.

Again, any cosmic ray events that interfered with subsequent analysis were removed manually.

As the UVES dataset was obtained to extend our study to higher  $v \sin i$  and fainter targets, some of these proved particularly difficult to analyze, and five were discarded leaving twelve for which atmospheric parameters and abundances have been estimated.

### 3.3. McDonald Observations

Fourteen runaway candidates were observed at the W. J. McDonald Observatory with the Tull coude echelle spectrograph at the 2.7m Harlan Smith telescope (Tull et al. 1995), with a high spectral resolution ( $R \approx 60,000$ ), during May and June 2013. Spectra were obtained covering a wavelength range 3,400–10,900 Å. The echelle data were split into orders, each of which was reduced separately using standard IRAF procedures.



For stars with significant rotational broadening and/or large surface gravities, the  $H\delta$  line profiles extended over a significant fraction of the order. Therefore, normalization of these data proved more difficult than those from UVES and FEROS. To deal with this, blaze fits were made to the bracketing orders, where the continuum was obvious, and these were averaged to provide a blaze profile for the order containing  $H\delta$ . This was then used to rectify the orders containing  $H\delta$ . All data were subsequently normalized and multiple exposures combined using either a median or weighted  $\sigma$ -clipping algorithm, within IDL, as above.

Three of the McDonald targets were not analyzed. HD 69686 and HD 118246 did not have sufficient SNR to identify the rotationally broadened Si III lines, preventing estimates of the projected rotational velocities, effective temperatures and microturbulences. HD 203664 had complex and variable spectra (Aerts et al. 2006) and so was removed from the sample.

#### 4. METHOD OF ANALYSIS

Non-LTE model atmosphere grids and model atoms from the TLUSTY and SYNSPEC codes (Hubeny 1988; Hubeny & Lanz 1995; Hubeny et al. 1998; Lanz & Hubeny 2007) were used to derive atmospheric parameters and chemical abundances. More detailed discussions of our analysis methods can be found in Hunter et al. (2007), while those of the atmospheric grids are in Ryans et al. (2003) and Dufton et al. (2005)<sup>7</sup>. Hence only a brief summary is given here.

Model atmosphere grids have been generated with metallicities representative of the Galaxy ( $[\log \text{Fe}/\text{H}] + 12] = 7.5$  dex, and other abundances scaled accordingly). These model atmospheres cover a range of effective temperatures from 12 000 K to 35 000 K in steps of 500 – 1500 K, and surface gravities ranging from close to the Eddington limit to 4.5 dex in steps of 0.15 dex (Hunter et al. 2008).

The codes make non-LTE assumptions, i.e. the atmospheres can be considered plane parallel with winds having no significant effect on the optical spectrum, and a normal helium to hydrogen ratio (0.1 by number of atoms) was assumed. Dufton et al. (2005) and McEvoy et al. (2015) independently tested the validity of this approach. They analysed the spectra of B-type supergiants in the SMC and LMC, respectively, using the grids described here and also the FASTWIND code (Santolaya-Rey et al. 1997; Puls et al. 2005) which incorporates wind effects. Dufton et al. (2005) found excellent agreement in the atmospheric parameters estimated from the two methods. Effective temperature, logarithmic surface gravity, and microturbulent velocity estimates all agreed to well within their errors. Abundance values agreed to within 0.1 dex for elements such as C, O, Si and Mg, while discrepancies in N abundances were less than 0.2 dex, although a systematic difference of 0.1 dex did appear to exist between the two approaches. Dufton et al. (2005) suggested that this was due to differences in the N model atoms and wind effects adopted. McEvoy et al. (2015) also found good agreement between results from the two codes. Of the eleven stars analysed using both methods, five targets had effectively identical results, five agreed well (with differences  $\leq 1000$  K in  $T_{\text{eff}}$ ,  $\leq 0.1$  dex in  $\log g$ , and  $\leq 0.2$  dex in N abundance estimates), with the N abundance in only one target showing significant discrepancies between the methods. However, this star is an

extreme object, close to the Eddington limit, where N abundances will be less secure. As the majority of our sample are lower luminosity dwarfs or giants, our approach should be adequate.

We adopt baseline chemical abundances from Hunter et al. (2007, 2009) derived from a sample of B-type stars in the Milky Way. Other B-type stellar studies, such as those by Lyubimkov et al. (2005, 2013); Daflon et al. (2009); Simón-Díaz et al. (2010); Nieva & Simón-Díaz (2011), have found higher baseline abundances for Mg, Si and N, closer to Solar abundances, but to maintain consistency in our analysis, we use the Hunter baseline values which for N, Si and Mg, are 7.62, 7.42 and 7.25 dex, respectively (see Hunter et al. 2007, 2009).

It is important to note that the stellar metallicity distribution in a disk galaxy, including the Milky Way, typically exhibits a negative gradient as a function of distance from the Galactic centre, both in the radial and vertical directions (Huang et al. 2015). Examples of studies where radial N abundance gradients in the Galactic disk have been studied include Rolleston et al. (2000), who found a gradient of  $-0.09 \pm 0.01$  dex  $\text{kpc}^{-1}$ , while Daflon & Cunha (2004) found an average gradient for all elements in the Galactic disk of  $-0.042 \pm 0.007$  dex  $\text{kpc}^{-1}$ , with an N value of  $-0.046 \pm 0.011$  dex  $\text{kpc}^{-1}$ , half of that estimated by Rolleston et al. (2000). Both of these measurements rely on abundances in young OB-type stars. Shaver et al. (1983) used radio and optical spectroscopy to sample Galactic H II regions, spanning 3.5–13.7 kpc from the Galactic centre. They found a N abundance gradient of  $-0.09 \pm 0.015$  dex  $\text{kpc}^{-1}$ , similar to Rolleston et al. (2000), along with evidence of steeper gradients in the inner regions of the Galactic disk. Huang et al. (2015) investigated this effect both radially and vertically using 7000 Red Clump stars between 7 and 14 kpc from the Galactic centre. They found that between 7 and 11.5 kpc the radial gradient flattens as the height from the Galactic plane increases, but that between 11.5 and 14 kpc the gradients do not vary with height and are at a constant value of  $-0.014$  dex  $\text{kpc}^{-1}$ . Rolleston et al. (2000) also considered a two-zone model, but found no evidence to indicate this was more appropriate. Here, an average N abundance for Galactic B-type stars has been adopted from Hunter et al. (2009), although this value may be slightly higher if stars were formed closer to the Galactic centre, and lower if formed far from it. However, in no case has the gradient been found to be very large, and so the metallicity distribution should not have a significant effect on the results presented here.

##### 4.1. Atmospheric parameters

The three characteristic parameters of a static stellar atmosphere (effective temperature, surface gravity and microturbulence) are inter-dependent and so an iterative process was used to estimate these values (see Fraser et al. 2010; McEvoy et al. 2015, for more details). The parameters are described separately below. The final values for these parameters are given in Table 3.

###### 4.1.1. Effective Temperature

Effective temperature ( $T_{\text{eff}}$ ) estimates were determined using the Si ionisation balance. Equivalent widths of the Si III multiplet (4552, 4567, 4574 Å) were measured, together with those for the Si IV lines at 4089 and 4116 Å in the hotter targets, and those of Si II at 4128, 4130 Å in the cooler stars.

<sup>7</sup> See also <http://star.pst.qub.ac.uk>

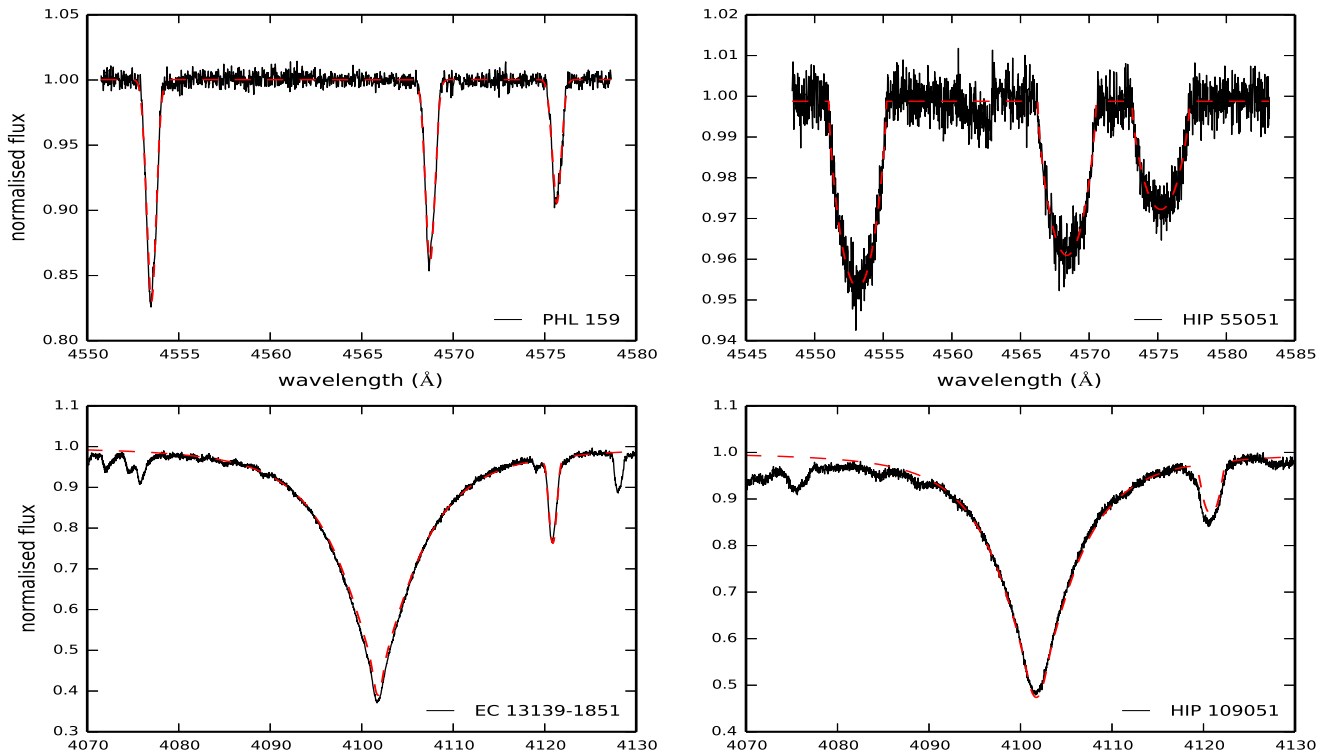


FIG. 1.— Upper left: Si III spectrum for PHL 159 ( $v \sin i = 30 \text{ km s}^{-1}$ ), with gaussian model fits (red dotted line) used to determine  $v_t$  and  $T_{\text{eff}}$ . Upper right: Si III spectrum for HIP 55051 ( $v \sin i = 135 \text{ km s}^{-1}$ ), with rotationally broadened model fits (red dotted line) used to determine  $v_t$  and  $T_{\text{eff}}$ . Lower left: H  $\delta$  spectrum for EC 13139-1851 ( $v \sin i = 43 \text{ km s}^{-1}$ ), along with its model fit, used to determine  $\log g$ . Lower right: H  $\delta$  spectrum for HIP 109051 ( $v \sin i = 108 \text{ km s}^{-1}$ ), along with its model fit, used to determine  $\log g$ .

For narrow lined, high signal-to-noise ratio targets, a simple Gaussian profile fit was sufficient to obtain a reliable equivalent width measurement (see Fig 1, upper left plot). The uncertainties in these measurements are typically of the order of 10% (Hunter et al. 2007). For stars with higher projected rotational velocities ( $v \sin i \geq 50 \text{ km s}^{-1}$ ), it was more appropriate to fit rotationally broadened profiles, as rotation becomes the dominant broadening mechanism (see Fig 1, upper right plot). In some cases it was not possible to measure the strength of either the Si II or Si IV spectrum. For these targets, upper limits were set on their equivalent widths, allowing constraints to the effective temperatures to be estimated (see, for example, Hunter et al. 2007, for more details). This was mostly the case for stars with large projected rotational velocities and mid-range temperatures (18,000 – 26,000K). The random uncertainty in our effective temperatures are approximately  $\pm 1000 \text{ K}$  (about 5%), consistent with the high quality of the observational data. In those cases where upper limits have been set for the equivalent widths of the Si absorption lines, the values will obviously be more uncertain and so error bars of  $\approx 2000 \text{ K}$  are more appropriate.

#### 4.1.2. Surface Gravity

The logarithmic surface gravity ( $\log g$ ) was estimated by comparing theoretical and observed profiles of the hydrogen Balmer line H $\delta$ . Automated procedures were developed to fit the theoretical spectra to the observed lines, with regions of best fit defined using contour maps of  $\log g$  against  $T_{\text{eff}}$ . Using the effective temperatures deduced by the methods out-

lined above, the gravity could be estimated. The effects of instrumental, rotational and macroturbulent broadening, which have most significant effect on the line cores, were considered in the theoretical profiles (see Fig 1, lower plots). Uncertainties in the fitting procedures led to random errors of  $\pm 0.1 \text{ dex}$ , while systematic errors could be present due to, for example, the uncertainty in the adopted line broadening theory or in the model atmosphere assumptions. Additional errors may arise from the uncertainty of the identification of the continuum around H $\delta$  in the McDonald spectra (see section 3.3), where less continuum was available around the line.

#### 4.1.3. Microturbulence

Following standard practice, we derived the microturbulent velocity from the Si III triplet (4552, 4567 and 4574  $\text{\AA}$  - see upper plots in Fig 1) as it is observed in all our analysable spectra and because all three lines arise from the same multiplet, so that errors in the absolute oscillator strengths and non-LTE effects should be minimized.

An alternative approach to the microturbulence determination uses the same Si III triplet but finds the microturbulence that gives the baseline Si abundance of 7.42 from Hunter et al. (2009) as the average from the three lines. This alternative impacts also the determination of the effective temperature and surface gravity and, hence, the abundances of all elements. In the next section, we comment on the effect on the abundances of the two methods for determining the microturbulence.

## 4.2. Elemental abundances

TABLE 3  
FINAL ATMOSPHERIC PARAMETERS FOR EACH STAR, LISTED BY HIP NUMBER, WITH ANOTHER IDENTIFIER SHOWN. EFFECTIVE TEMPERATURES, SURFACE GRAVITIES AND  
MICROTURBULENCES ARE GIVEN FOR EACH STAR, ALONG WITH MAGNESIUM, SILICON, NITROGEN AND CARBON ABUNDANCES WHERE AVAILABLE<sup>a</sup>.

HIP	Other	$T_{\text{eff}}$ K	$\log g$ cm-s <sup>-2</sup>	$v_t$ km-s <sup>-1</sup>	Mg	Si	N	C
2702	HD 3175	16100	3.6	8	6.85	7.02	7.35	7.82
3812	CD -56 152	17000	3.4	14	6.83	6.83	7.42	...
7873	HD 10747	18700	3.8	8	7.03	7.01	7.33	7.69
13489	HD 18100	23500	3.6	15	7.05	6.64	7.42	...
16758	HD 22586	21700	3.3	14	7.44	7.62	7.93	8.13
45563	HD 78584	18600	3.8	8	7.01	6.81	7.31	...
55051	HD 97991	21500	3.8	5	6.98	7.36	7.58	...
56322	HD 100340	24500	3.8	4	7.43	7.55	7.61	...
60615	BD +36 2268	19600	3.4	9	6.97	6.82	7.66	...
61431	HD 109399	23000	3.1	16	7.38	7.24	7.42	...
64458	HD 114569	18300	3.8	6	7.21	7.24	7.90	8.39
67060	HD 119608	19900	2.7	16	7.52	7.67	7.93	8.05
68297	HD 121968	20550	3.4	0	7.43	7.98	7.72	...
70205	LP 857-24	24600	4.1	0	7.45	7.46	7.42	...
70275	HD 125924	21000	3.6	6	7.08	7.13	7.28	...
79649	HD 146813	19400	3.2	5	7.02	7.25	7.47	...
81153	HD 149363	27800	3.5	12	7.60	7.79	7.86	8.22
85729	HD 158243	19300	2.7	20	7.37	7.69	7.91	8.02
91049	HD 171871	20300	3.4	14	7.35	7.51	7.81	...
92152	HD 173502	25600	3.5	12	7.51	7.74	7.98	...
94407	HD 179407	26000	3.4	17	8.00	7.82	8.21	8.53
96130	HD 183899	20000	3.3	17	7.18	7.53	7.80	7.98
98136	HD 188618	21300	3.4	11	7.32	7.34	7.85	...
101328	HD 195455	20550	3.2	14	7.47	7.74	7.96	7.83
105912	HD 204076	20100	3.4	20	7.19	7.43	7.97	-
107027	HD 206144	17750	2.5	16	7.24	7.31	7.56	7.68
109051	HD 209684	20340	3.9	9	6.98	7.17	7.54	...
111563	HD 214080	19400	2.9	17	7.18	7.63	7.56	7.81
112022	HD 214930	18000	3.4	6	7.04	7.04	7.27	...
112482	HD 215733	23100	2.9	14	7.39	7.40	7.60	...
113735	HD 217505	21600	3.9	3	7.27	7.33	7.56	7.97
114690	HD 219188	23200	3.0	13	7.37	7.71	7.66	7.86
115347	HD 220172	21700	3.8	0	7.31	7.41	7.69	7.95
115729	HD 220787	18600	3.6	5	7.01	7.07	7.51	7.91
...	EC 05582-5816	15900	3.4	10	6.97	7.43	8.40	8.39
...	EC 13139-1851	18100	3.9	13	7.09	7.21	7.64	...
...	EC 20140-6935	21900	3.8	0	7.20	7.47	7.72	8.09
...	PB 5418	19300	3.8	8	7.05	7.07	7.44	...
...	PHL 159	22900	4.1	0	7.46	7.41	7.46	...

<sup>a</sup> Analysis of EC 05582-5816 is based on model atmospheres with the Si abundance set to 7.4. For all other analyses, the Si abundance is determined from silicon lines and the microturbulence from the Si III lines.

Nitrogen, magnesium, silicon, and in some cases carbon abundances for each star have been estimated using the atmospheric parameters given in Table 3 and measurements of absorption lines. Abundances are given in Table 3. The atmospheric parameters agree well between observations with the different spectrographs. Effective temperatures show differences not larger than 1200 K in all cases, while the range of the logarithmic gravity estimates is only greater than 0.2 dex in one instance (HD 121968 with a range of 0.25 dex). Differences in microturbulence are less than 6 km s<sup>-1</sup> in all cases. The agreement between atmospheric parameters derived from observations obtained with different instruments is reassuring but not surprising given the high-quality of all spectra. This agreement is, of course, not a measure of any systematic errors.

Extensive appendices in Hunter et al. (2007) show how errors in the atmospheric parameters for B-type stars translate into errors in derived abundances. Hunter et al. considered

the errors to be independent but in reality the situation will be more complicated, as this is not the case. For example, an increase in the effective temperature estimate will lead to an increase in the gravity estimate and this leads to the theoretical N II equivalent widths (and hence nitrogen abundances) being less sensitive to changes in the atmospheric parameters than if these are considered to vary independently.

For the range in atmospheric parameters found for our sample, the simulations of Hunter et al. imply (see for example their Fig. 6 for the N II 3995 Å line) that our estimated errors in both the gravity and microturbulence lead to relatively small errors in the nitrogen abundance estimate of 0.1 dex or less. Errors in effective temperature estimates are more important and lead to larger uncertainties with an error of  $\Delta T_{\text{eff}} \pm 1000\text{K}$  translating into a nitrogen abundance error of approximately  $\mp 0.2$  dex at an effective temperature of 18000 K but decreasing to  $\sim 0.1$  dex at an effective temperature of 25000 K. Additionally there will be random errors in the ni-

trogen abundance estimates due to uncertainties in the N II equivalent widths. The latter have been estimated as  $\pm 10\%$  which would imply an uncertainty of  $\sim 0.1$  dex. Combining these different sources of error in quadrature would lead to typical uncertainties of 0.2-0.3 dex.

For the atmospheric parameters and abundances in Table 3, the microturbulence was derived from the three Si III lines with the condition that the three lines return the same  $\text{Si}^{2+}$  abundance. This method was successful for all but EC 05582-5816 for which lines are greatly rotationally broadened. As we noted above, the alternative method is to assume a standard Si abundance of 7.4 for the determination of the microturbulence and, hence, other atmospheric parameters which finally define the model atmosphere used to determine the abundances of C, N and Mg. (This alternative method was used by Hunter et al. (2007) in their analysis of B stars in three Galactic clusters.) The C, N and Mg abundances are little affected by how the microturbulence is chosen; the preferred and alternative methods give similar results. This is well shown by Figure 2 where we show the N abundances obtained when the microturbulence is set by the condition that the Si abundance is 7.4 plotted versus the abundances obtained when the microturbulence comes from the three Si III lines. It is seen that the N abundances are not systematically different in the two cases except for two or three outliers. Obvious outliers are HD 18100 and BD +36 2268 with N abundances from the alternative method of 7.97 and 8.20, respectively. A similar correspondence between abundances from the two methods is found for Mg and the limited number or determinations of the C abundances. Thus, apart from the artificial constraint of a constant Si abundance, the abundance analyses for all other elements are expected to be largely unaffected by the method used to determine the microturbulence and, hence, the atmospheric parameters.

For a subsample of our stars (all stars observed with FEROS) we estimated carbon abundances. The C II line at  $4267 \text{ \AA}$  was used to calculate abundances as it is the only measurable line in all of the spectra. This line is known to be susceptible to (subtle) non-LTE effects (Nieva & Przybilla 2006, 2008), which are not fully taken into account in the model ion that was included in the TLUSTY calculations - see discussion by Hunter et al. (2009). Our interpretation (see below) of the various abundances is in part referenced to the abundance analysis of Galactic cluster by Hunter et al. (2007) who used also exclusively the  $4267 \text{ \AA}$  line and, thus, the inability to account fully for the non-LTE effects should be almost cancelled by the comparison with the Galactic clusters.

Nitrogen abundances in Table 3 were estimated from the singlet transition at  $3995 \text{ \AA}$  as it is one of the strongest N II lines in the optical spectrum and appears unblended. Two examples of spectra of high  $v \sin i$  stars around the N line at  $3995 \text{ \AA}$  are shown in Figure 3. Other N II lines were also present in a significant number of observations, including those between  $4601$  and  $4643 \text{ \AA}$  and the singlet at  $4447 \text{ \AA}$ . These tended to be more blended, and so may lead to less accurate abundance estimates than those from  $3995 \text{ \AA}$ . It is interesting to note that Lyubimkov et al. (2013) found that the line at  $3995 \text{ \AA}$  gave a lower N abundance in their sample compared with the abundance from other transitions and that the differences were a function of effective temperature ranging from  $-0.3$  dex at  $16000 \text{ K}$  to  $0.0$  dex at  $29000 \text{ K}$ . In our case, the difference is about  $-0.1$  dex over the full tem-

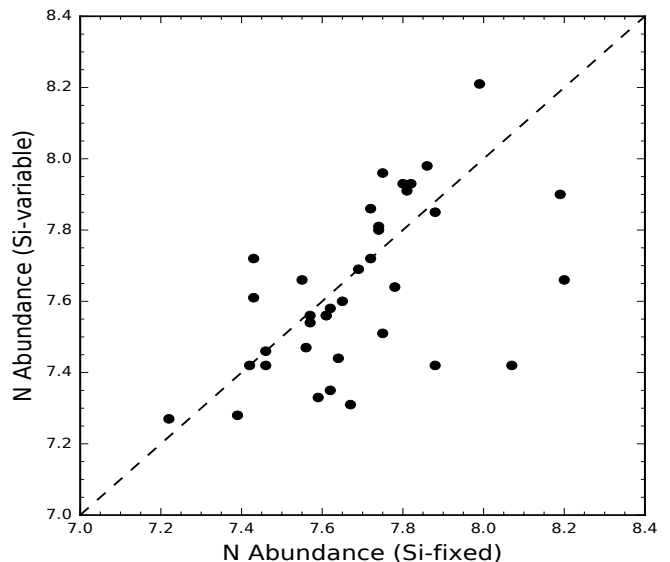


FIG. 2.— Nitrogen abundances from models with the microturbulence set by the condition that the Si abundance is 7.40 versus the N abundances set by determination of the microturbulence from the Si III lines. The solid line of unit slope corresponds to an abundance independent of the method of fixing the microturbulence.

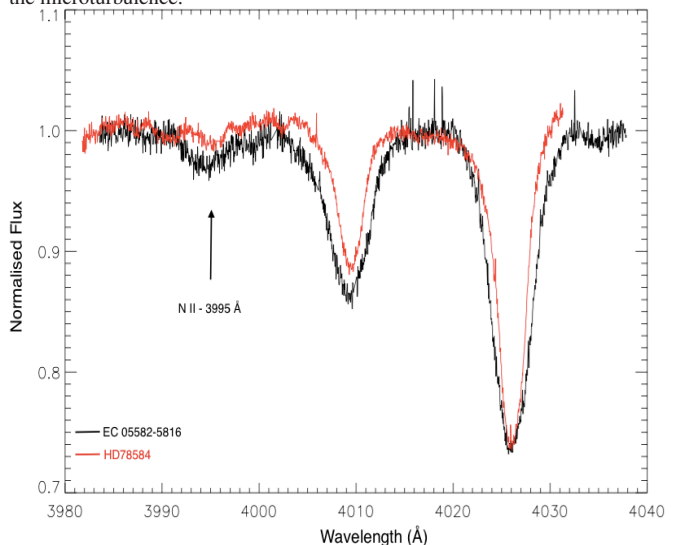


FIG. 3.— The spectrum around the N II line at  $3995 \text{ \AA}$  for the most nitrogen enhanced star, EC 05582-5816. HD 78584 is over-plotted in red for comparison, as it has similar spectral type (B3) and  $v \sin i$  of  $102 \text{ km s}^{-1}$ . Although the nitrogen line is heavily broadened in EC 05582-5816, due to its very high  $v \sin i$  of  $221 \text{ km s}^{-1}$ , it can still clearly be seen, so has to be particularly strong to avoid being smeared out into the surrounding continuum.

perature range with a rise to  $0.0$  dex below about  $18000 \text{ K}$ . These differences with Lyubimkov et al. (2013) likely reflect differences in the adopted model atoms. By referencing our abundances from the  $3995 \text{ \AA}$  line to those from Hunter et al. (2009), we expect to obtain a true measure of abundance differences between the cluster (i.e., Galactic disk) and runaway B stars.

Magnesium abundances were estimated for all spectra using the Mg II transition at  $4481 \text{ \AA}$  comprising three overlapping lines of a single multiplet.

Silicon abundances are obtained from the lines of Si II, Si III and Si IV referred to in the determination of the atmospheric



parameters.

## 5. EJECTION MECHANISMS AND ABUNDANCES

The most satisfying discussion of the abundances would conclude with the demonstration that runaway B stars formed by the BSS and the CES have distinct differences in composition with both scenarios providing abundances differences with B stars in Galactic open clusters. Perhaps the least satisfying result would be one in which the runaway B stars showed a common pattern of abundances and one which matched well the abundances of the B stars in Galactic open clusters, i.e., the BSS and CES scenarios both preserve the abundances of the investigated elements. Yet in this case, the origin of runaway stars may hopefully be traced from other observational indicators such as binarity and rotational velocities.

The X-ray sources known as low-mass X-ray binaries (LMXBs) consist of a low mass “normal” secondary star orbiting a black hole (BH) or a neutron star (NS) where the supernova leading to the BH or NS likely contaminated the secondary. Abundance analysis of the secondary should offer clues to the contamination expected in the BSS mode of runaway star formation. One LMXB secondary accompanying a BH has a spectral type of B9III and with an effective temperature of 10500 K approximates a runaway star. With  $[\text{Fe}/\text{H}] = 0.0$ , this secondary in V4641 Sgr has a normal composition (C, O, Mg, Al, Si and Ti) but an +0.8 dex overabundance for N and Na (Sadakane et al. 2006). Curiously, this star appears to be a replica of EC 05582-5816 (see Section 5.3). Unfortunately C and N abundances have not been reported for the other six LMXB secondaries. The secondary with the most extreme enrichments would appear to be Nova Sco 1994 (González Hernández et al. 2008) with, for example,  $[\text{Fe}/\text{H}] = -0.1$  but  $[\text{Mg}/\text{Fe}] = +0.4$  and  $[\text{Si}/\text{Fe}] = +0.7$  and other anomalies including  $[\text{O}/\text{Fe}] = +1.0$  and  $[\text{S}/\text{Fe}] = +0.9$ . Mg and Si abundance estimates are available for five secondaries. Comparisons with normal F, G and K dwarfs are made in the  $[\text{Fe}/\text{H}]$  versus  $[\text{X}/\text{Fe}]$  plane where  $\text{X} = \text{Mg}$  or  $\text{Si}$ . The mean  $[\text{Fe}/\text{H}]$  for the five stars is +0.1 with a spread from -0.1 to +0.3. The mean difference with respect to normal stars of the same  $[\text{Fe}/\text{H}]$  is  $[\text{Mg}/\text{Fe}]$  and  $[\text{Si}/\text{Fe}]$  at +0.2 with a spread from 0.0 to about +0.7 but the Mg and Si enrichments would be larger if Fe were also enriched. There is a hint that  $[\text{Mg}/\text{Fe}]$  and  $[\text{Si}/\text{Fe}]$  are positively correlated. Other elements considered for four or more of the secondaries but not included in our analysis include the following with mean differences of  $[\text{X}/\text{Fe}]$  relative to normal stars: +0.4 (O), +0.4 (Na), +0.1 (Al), 0.0 (Ca), +0.2 (Ti) and +0.1 (Ni), again elemental abundance enrichments are larger if supernova Fe contaminates the secondary. Predicted enrichments depend on many factors including uncertain aspects of the SN explosion and do not completely account for the composition of these secondaries. In summary, as far as the elements considered here are concerned, observations of C and N are too few to suggest a pattern but Mg and Si may be enriched simultaneously in some cases.

Possible changes of composition occurring at the birth of a runaway star have to be extracted from the observed composition bearing in mind that two other factors may affect the chemical composition of the B stars prior to their conversion to a runaway star: First, the initial composition of B (and other) stars depends on the location of their birth site; studies of the composition of stars and H II regions show that abundances decline with increasing distance from the Galactic

center. For example, Daflon & Cunha (2004) from B stars and Luck & Lambert (2011) from Cepheids find that the abundance gradients for our elements are about  $-0.045 \text{ dex kpc}^{-1}$ , a value representative of many other studies. Azimuthal variations are considered to be smaller than the radial variation. Since runaway stars in the sample catalogs are expected to have birth sites spanning several kpc in the Galactic disk, abundance variations of several 0.1 dex may be anticipated. Second, B stars may be prone to mixing between the surface and the interior resulting in changes of composition as CN-cycled H-burning products reach the atmosphere, i.e., the He/H ratio is increased with a coupled decrease of C and an increase of the N abundance -see, for example, calculations of surface abundances along evolutionary tracks for rotating massive stars by Brott et al. (2011). (Extreme mixing may contaminate the atmosphere with ON-cycled H-burning products resulting in decreases of O and additional increases of N and He.)

### 5.1. Magnesium and Silicon

Since the Mg and Si abundance should be unaffected by mixing within evolving B stars but could conceivably be altered in runaway stars created by the BSS, we discuss this pair of elements ahead of our discussion of C and N. Our reference Galactic B stars are the three open clusters analyzed by Hunter et al. (2009): NGC 6611 at a Galactocentric distance  $R_G$  of 6.1 kpc, NGC 3293 at  $R_G = 7.6$  kpc and NGC 4755 at  $R_G = 8.2$  kpc where  $R_G$  is taken from Rolleston et al. (2000). (Daflon & Cunha (2004) give somewhat different estimates.) Abundances provided by Hunter et al. (2009) correspond to atmospheric parameters chosen by assuming a Si abundance of 7.4 (see above for comments on such a choice). Since the 2.1 kpc difference in Galactocentric distance across the three open clusters should correspond to an abundance difference of only about 0.09 dex, assumption of constant Si abundance is likely not a source of significant systematic error. The Mg abundances for the three Galactic clusters are just consistent with the anticipated 0.09 dex decline between NGC 6611 and NGC 4755. Of course, the Si abundances are not expected to betray the abundance gradient because the condition  $\text{Si} = 7.4$  was imposed on the analysis.

For the runaway B stars, the Mg and Si abundances from Table 3 are compared in Figure 4 which shows that Mg and Si abundances are highly correlated and each range over 1.0 dex. The straight line in Figure 4 corresponds to a constant Mg/Si ratio set at the ‘standard’ ratio of -0.17 dex adopted by Hunter et al. (2009). The spread in Mg abundances among the runaway stars far exceeds the range among stars from an individual open cluster which is a fair measure of the measurement uncertainties given that stars within a cluster share a common Mg abundance. A major contribution to the Mg and Si abundance spread among the runaway stars surely arises because their birthplaces span quite a range in Galactocentric distances even though present Galactocentric distances may not be too different, a range much greater than the range spanned by the three reference open clusters. Indeed, Galactic orbits calculated by Silva & Napiwotzki (2011) give birthplaces from the Galactic center out to nearly 14 kpc for the sample drawn from their paper. However, plots of the Mg and Si abundances versus the estimated Galactocentric distance of a star’s birthplace are too ill-defined to confirm the abundance gradients obtained from *in situ* abundance measurements of young stars and H II regions. All but three of our stars have estimated birthplaces between 4 kpc and 10 kpc. The fail-



ure to reproduce the observed abundance gradients may be attributable to uncertainties in the locations of the birthplaces and to contamination of the stars in the BSS by Mg and Si from the supernova.

Scatter in Figure 4 about the linear relation is consistent with Mg and Si abundance uncertainties and with the spread in Mg abundances within each of the open clusters (see below). Presence of the linear correlation and a constant Mg/Si ratio is qualitatively expected from the similar nucleosynthetic yields of Mg and Si from Type II supernovae which are surely the controlling influence on the Galactic abundance gradient whatever the influence of the myriad other factors (e.g., the initial mass function, the star formation rate, Galactic infall etc.) entering recipes for Galactic chemical evolution.

### 5.2. Carbon and Nitrogen

Among the B stars in the three reference clusters, Hunter et al. (2009) found that the C and N abundances were independent of position on a star's evolutionary track except that half of the few supergiants were enriched in CN-cycled material. Similarly, Lyubimkov et al. (2013) found normal C and N abundances in a sample of 22 slightly-evolved B stars (i.e., no supergiants) except for two possibly mixed stars. Thus, the expectation is that the majority of the B stars before undergoing conversion to a runaway star would have preserved their initial C and N abundances. The likely corollary of this expectation is that alterations to the C and N abundances may be clues to the process creating the runaway star but internal CN-cycling and mixing to the surface may have occurred independently of formation as a runaway star.

As noted above, C abundances in Table 3 are provided only for the stars observed with FEROS. Figure 5 shows the C and N abundances for this minority. C and N abundances for EC 05582-5816 in Table 3 unlike for other stars are taken from an analysis with the Si abundance fixed at 7.4 but, as noted above, the C and N abundances are expected to be independent of this assumption concerning the Si abundance; the high  $v \sin i$  of EC 05582-5816 precluded the use of the Si III multiplet to determine the microturbulence. The C and N abundances are tightly correlated with all stars showing a similar C/N ratio to within the measurement uncertainties. In addition, the three Galactic clusters analysed by Hunter et al. (2009) have mean C and N abundances falling within the band defined by the runaway stars, that is mean abundances of  $8.00 \pm 0.19$  and  $7.62 \pm 0.12$  for C and N, respectively, for all non-supergiants in the three Galactic clusters with these abundances provided by analyses assuming Si has its standard abundance.

These carbon abundances for the subset of our runaway stars show no evidence for a runaway star enriched in CN-cycled material, i.e., a low C abundance paired with a high N abundance such that the total number of C and N atoms is conserved. Very severe contamination with CN-cycled material would result in a N enrichment of up to 0.5-0.6 dex and a severe depletion of C. No such stars are seen in Figure 5. Presence of CN-cycled material may occur in the B star prior to its conversion to a runaway star and is, thus, not a determining signature of a process resulting in a runaway star.

### 5.3. Nitrogen and magnesium

To extend the search for abundance anomalies to the complete sample, we examine next the relationship between the N

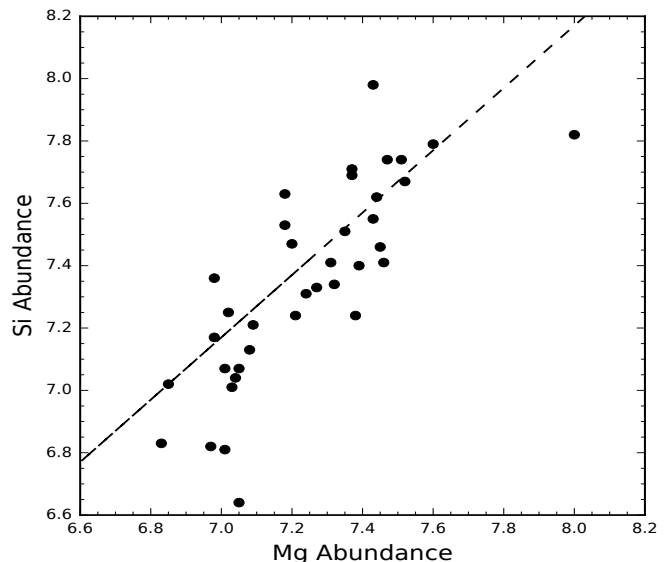


FIG. 4.— Mg and Si abundances from Table 3. The straight line corresponds to a Mg/Si ratio of  $-0.17$  dex normalized to the standard abundances adopted by Hunter et al. (2009).

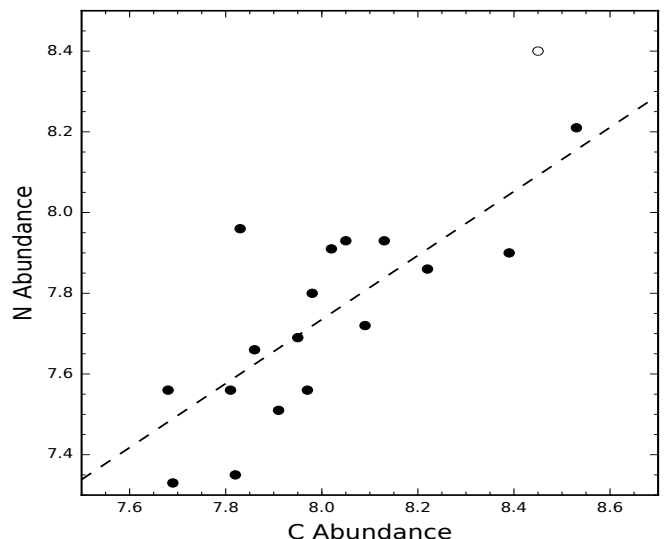


FIG. 5.— C and N abundances plotted for the FEROS sample of runaways. Abundances are taken from Table 3. The straight line, a least-squares fit, shows that C and N abundances are related over a range of about 1 dex with a scatter consistent with measurement uncertainties, i.e., there are no stars heavily contaminated with CN-cycled products, that is stars which are C-poor and N-rich. Data for EC 05582-5816 (open circle) are taken from the analysis in which the Si abundance is fixed at 7.4.

and the Mg abundances. Figure 6 drawing on Table 3 compares the N and Mg abundances with a distinction made according to surface gravity (i.e., evolutionary status) with stars with  $\log g < 3.2$  (i.e., supergiants) represented by open circles and stars of higher surface gravity (i.e., main sequence and slightly evolved stars) represented by filled circles. Figure 7 shows the N and Mg abundances for B stars belonging to the cluster NGC 3293, the best represented of the three clusters studied by Hunter et al. (2009).

With the possible exception of N enrichment from internal mixing or mass loss, one expects the cluster's stars in Figure 7 to share the same N and certainly the same Mg abundance. Thus, the scatter in N and Mg abundances in Figure 7 rep-

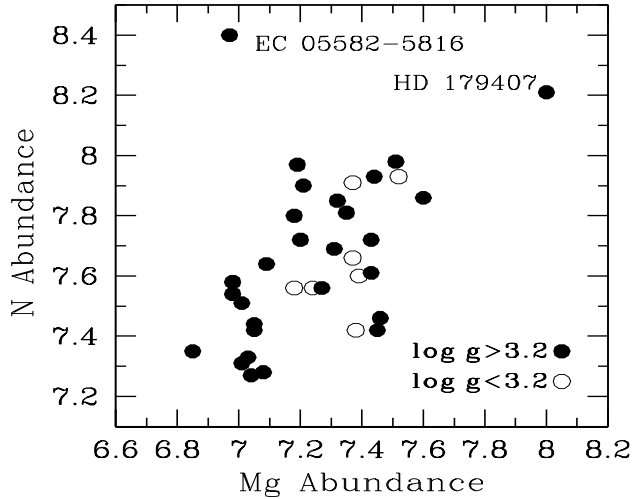


Fig. 6.— Mg and N abundances from Table 3 with stars distinguished by their surface gravity:  $\log g > 3.2$  shown as filled circles and  $\log g < 3.2$  shown as unfilled circles. Two outliers are identified — EC 05582-5816 and HD 179407 — and discussed in the text.

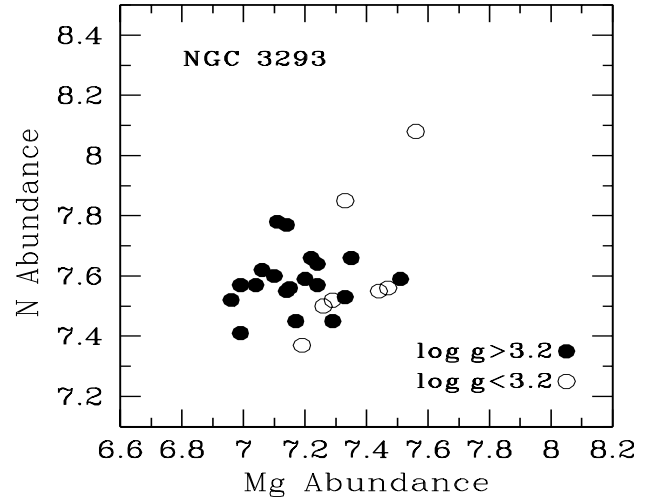


Fig. 7.— Mg and N abundances for B stars in the open cluster NGC 3293 with data from Hunter et al. (2009). Stars are distinguished by their surface gravity — see caption to Figure 6.

resents the measurement uncertainties which, thanks to the similarity of analytical techniques, will be a very close approximation to the uncertainties affecting the points in Figure 6. (One star — a supergiant — in NGC 3293 appears N-enriched but this star is not C-depleted.) Comparison of Figures 6 and 7 shows that the spread shown by NGC 3293’s B stars and, hence, we conclude that the runaways show an intrinsic star-to-star difference in composition (i.e., C, N, Mg and Si abundances but with similar abundance ratios) which we attribute to differences in a star’s birthplace with the Galactic abundance gradient being a very likely controlling factor.

EC 05582-5816 and HD 179407 appear as outliers in Figure 6. The two outliers have similar compositions but for their Mg abundances and both appear related to the inner Galaxy. Silva & Napiwotzi (2011) estimate EC 05582-5816’s birthplace at 2 pc from the Galactic centre. HD 179407 is presently at  $R_G = 3.5$  kpc according to Smartt et al. (1997). The pair have very similar C and N abundances (Table 3) but differ substantially in Mg with an abundance of 8.0 for HD 179407 but 7.0 for EC 05582-5816. The Si abundance of HD 179407 is consistent with its Mg abundance. For EC 05582-5816, present analysis assumes a Si abundance of 7.4. Galactic abundance gradients likely account for the high abundances found for HD 179407. There is a remarkable similarity in composition between EC 05582-5816 and the B9 III secondary of the black hole binary V4641 Sgr. This B star has  $[\text{Fe}/\text{H}] = 0$  and normal abundances of C, O Mg, Al Si and Ti but a high N and Na overabundances ( $[\text{N}/\text{H}] = [\text{Na}/\text{H}] = +0.8$ ) (Sadakane et al. 2006). If placed in Figure 6, it would provide a third outlier and fall near the two existing outliers! Reobservation and re-analysis of EC 05582-5816, a rapid rotator is to be encouraged and extended to additional elements.

#### 5.4. Formation mechanisms and Abundance Anomalies?

Nitrogen, magnesium and silicon abundances across the sampled runaway B stars are similar to those seen in B stars in Galactic clusters. The spread in the C, N, Mg and Si abundances and the nearly uniform abundance ratios C/N/Mg/Si among runaway stars in our sample results from the combi-

nation of two facts: (i) the stars’ birthplaces sample a wide range in Galactocentric distances and (ii) the abundances in star-forming regions decline with increasing Galactocentric distance at a rate of approximately  $0.05$  dex  $\text{kpc}^{-1}$ . Within our sample, there are no certain outliers with abundance peculiarities. Thus, the conclusion is that the two scenarios — BSS and CES — capable of ejecting B (and other) stars from the Galactic disk into the Galactic halo do not as a rule change the surface chemical composition of the runaway star, as sampled by C, N, Mg and Si. This conclusion from our non-LTE analysis confirms earlier LTE analyses in which the compositions of a runaway star and a comparable B star in the Galactic disk are compared, see, for example, Martin (2004). Although changes may occur in rare cases, the general conclusion is both disappointing and challenging. Disappointing in that the composition, a readily obtainable quantity, appears not to be a discriminant between competing ejection mechanisms. Challenging in that other observable quantities now have to be relied upon to identify the principal ejection mechanism across a sample of runaway stars and for individual runaway stars. Possible observables include projected rotational velocities and binarity.

## 6. EJECTION MECHANISMS: ROTATIONAL AND RADIAL VELOCITIES

### 6.1. Projected rotational velocities

The distribution of projected rotational velocities  $v \sin i$  for our sample of runaways is very similar to that provided by the B stars in the three Galactic clusters observed by Hunter et al. (2009): velocities up to  $300 \text{ km s}^{-1}$  with a peak near  $50 \text{ km s}^{-1}$  and few slow rotators (say  $v \sin i \leq 30 \text{ km s}^{-1}$ ). Martin (2006) considered rotational velocities for his sample of runaways and found their frequency distribution to be similar to that assembled by Guthrie (1984) from “young” OB associations whose result is similar to that from the three Galactic clusters. In contrast, B stars in “old” associations and field B stars in the Galactic disk have distributions which rise with decreasing  $v \sin i$  (Wolff et al. 1982; Guthrie 1984). A more recent catalog of projected rotational velocities for 102 north-

ern B stars is provided by Abt et al. (2002).

Tying the  $v \sin i$  distribution of the runaways to the ejection mechanisms is unfortunately hampered by the absence of quantitative predictions for the BSS and CES. In the BSS, if the runaway originates in a close binary system, the runaway may be tidally locked resulting in the rotation velocity being closely related to its orbital velocity. In turn, the ejection velocity is expected to be related to the orbital velocity. These ideas, lead to the expectation that the ejection velocity should be positively correlated with the rotational velocity but, as Martin (2006) demonstrated runaway stars do not show the expected correlation and, therefore, the BSS is not the leading producer of runaway stars. For the CES, the likelihood of ejection is plausibly higher in denser environments. On this simple premise and the match between the  $v \sin i$  frequency distribution for runaways and “young” associations, Martin considered that it ‘seems likely that the [CES] is the dominant mechanism’ behind his runaway sample and by extension ours too which has overlap with his sample.

### 6.2. Radial velocities

In the BSS, the resulting runaway B star will be either a single B star or form a binary system with a low-mass compact companion (e.g., a neutron star). A runaway which is single will be paired with a distant ejected neutron star or a black hole moving in a generally opposite direction. Portegies Zwart (2000) suggests that 20% to 40% of the runaway B stars should be accompanied by a neutron star and, thus, the runaway B star should appear as a single-lined spectroscopic binary with a period of several hundred days.

In the CES, simulations (Leonard & Duncan 1990) suggest that 10% of the runaways will be binaries comprised of normal main sequence stars and likely observable as double-lined spectroscopic binaries.

A definitive test of these predictions for the BSS and CES will require both a radial velocity long-term survey of a large sample of runaway B stars to be put up against more precise predictions about the frequency and nature of the binary populations from the two scenarios. Then, it may be possible to assess in a statistical fashion the relative production rates from the BSS and CES. For the binaries, it should be possible to assign them to either the BSS (i.e., a neutron star/pulsar companion) or to the CES (i.e., a normal main sequence companion). For the runaway single stars, the attribution to the formation scenario will be difficult unless one can uncover a subtle abundance anomaly or apply precise determination of space motions (GAIA?) to assist in the identification of the pulsar or the original stellar association.

A definitive observational test is not possible at present. The sole radial velocity survey of high Galactic OB stars was conducted by Gies & Bolton (1986) who concluded that “runaway OB stars are deficient in close binaries by a factor of 2-4”. Their sample of 15 confirmed runaways provided two binaries (both double-lined systems) and, if five probable runaways are added, the binary probability becomes 2/20 or 10%. The deficiency of binaries is suggested by reference to the binary fraction of 31% among normal O stars (Garmany et al. 1980) and of 38% among normal B stars (Abt & Levy 1978). Five of our stars (HD 97991, 149363, 214930, and 219188) were in the Gies & Bolton survey and declared by them to have a constant radial velocity. Martin (2003) found the runaway HD 138503 to be a double-lined spectroscopic binary, a star in Silva & Napiwotzki’s list of runaway stars. HD 1999 and HD 204076 observed by us are double-lined bina-

ries. Two radio surveys for pulsars reported no detections coincident with runaway OB stars (Sayer et al. 1996; Philp et al. 1996). Unfortunately, the correction for the beaming of pulsar radiation results in an uninteresting limit on the fraction of runaway stars with low-mass compact companions; Sayer et al. estimate that less than 25-50% of OB runaways have a neutron star companion, an estimate consistent with the prediction by Portegies Zwart (2000).

Our sample can make only a modest contribution to the frequency of binary runaway stars as a test of the BSS and CES. For the majority of our sample, the star was observed once and an assessment of the radial velocity variation must come from velocities reported in the literature. Eight stars were observed at two or more telescopes and, thus, at different epochs and the two or three radial velocity measurements may be inter-compared and also checked against the literature. (This restricted search for velocity variations is akin to that reported by Martin (2006) who observed many runaway stars at least twice over a few days and also checked velocities against the literature.) We have defined a star with a radial velocity variation between measurements of greater than  $20 \text{ km s}^{-1}$  as a possible member of a binary system. This cut off is set by inspection of other studies of OB stars (Sana et al. 2013; Dunstall et al. 2015). In some stars, significant velocity variations arise from pulsations which complicates the search for orbital radial velocity variations and, if neglected as a source of radial velocity variations, the fraction of spectroscopic binaries is overestimated.

Radial velocities are provided in Table 4. Of the eight stars observed twice or thrice by us, seven appear to have a constant velocity. The star with a variable radial velocity is HD 204076 which is certainly a spectroscopic binary; the UVES but not the FEROS spectrum showed double lines. HD 219188 is possibly a variable. There is a  $25 \text{ km s}^{-1}$  difference between our two measurements and online catalogs give a velocity either close to the mean of our two or a less positive velocity:  $84 \text{ km s}^{-1}$  according to Silva & Napiwotzki (2011) or  $64 \text{ km s}^{-1}$  according to Gontcharov (2006) and Kharchenko et al. (2007).

Inspection of Table 4 suggests that four stars observed once by us may be binaries on account of a difference with radial velocities reported in the literature. EC 20140-6935 (HD 192273) was noted as a possible binary by Magee et al. (1998) who found a  $45 \text{ km s}^{-1}$  velocity difference between their measurement and that reported by Rolleston et al. (1997). Silva & Napiwotzki (2011) give the velocity as  $+17 \text{ km s}^{-1}$  from Rolleston et al. Our velocity is in good agreement with that by Magee et al. HD 188618 was suspected by Martin (2006) to be a binary from the velocity difference between his measurement of  $29 \pm 6 \text{ km s}^{-1}$  and a previous measurement of  $-15 \text{ km s}^{-1}$  by Dufflot et al. (1998). Our  $-46 \text{ km s}^{-1}$  extends the velocity range. HD 179407’s present and previous velocity measurements barely satisfy our  $20 \text{ km s}^{-1}$  condition. HIP 70205 (LP 857-24) exhibits a  $300 \text{ km s}^{-1}$  difference but the only previous measurement is from the RAVE survey (Kordopatis et al. 2013) which is possibly ill-suited to velocity measurements of B stars which provide few lines in the RAVE bandpass. Obviously, this star deserves further attention. Finally, there is HD 114569 which has no previous velocity measurement.

It seems fair to conclude that our sample contains few spectroscopic binaries and certainly fewer than the approximately 30% provided by a sample of field B stars in the Galactic disk (Abt & Levy 1984). Our sample is but very slightly biased by the exclusion of known double-lined or even single-lined

TABLE 4

EACH STAR LISTED BY HIP NUMBER ALONG WITH ALTERNATIVE IDENTIFIER, RADIAL VELOCITY FROM OUR ANALYSIS AND FROM THE LITERATURE (WITH REFERENCES) ALONG WITH THE BINARY STATUS OF THE STAR.

HIP	Other	Radial velocity		Ref <sup>b</sup>	Status
		Us <sup>a</sup>	Literature		
2702	HD 3175	-13±2 (F)	-16±3	R3	Single
3812	CD -56 152	14±8 (U)	19±10	R2	Single
7873	HD 10747	-9±2 (F)	-12±2	R1	Single
13489	HD 18100	80±7 (F)	76±3	R1	Single
16758	HD 22586	99±1 (F)	97±2	R3	Single
45563	HD 78584	-120±6 (T)	-125±2	R1	Single
55051	HD 97991	31±3 (U)	26±3	R3	Single
56322	HD 100340	253±10 (T), 263±4 (U)	254±9	R2	Single
60615	BD +36 2268	31±4 (T)	31±7	R3	Single
61431	HD 109399	-43±3 (F)	-49±2	R1	Single
64458	HD 114569	104±2 (F)	...		Unknown
67060	HD 119608	31±1 (F)	26±4	R1	Single
68297	HD 121968	17±9 (T), 29±3 (U)	28±2	R4	Single
70205	LP 857-24	243±4 (F)	-54±2	R5	Binary?
70275	HD 125924	244±1 (T)	239±2	R4	Single
79649	HD 146813	21±2 (T)	19±6	R4	Single
81153	HD 149363	145±3 (T), 146±3 (U), 144±3 (F)	141±2	R1	Single
85729	HD 158243	-63±2 (F)	-64±3	R1	Single
91049	HD 171871	-64±1 (T)	-62±5	R1	Single
92152	HD 173502	49±1 (F)	68±4	R1	Single?
94407	HD 179407	-120±4 (F)	-119±5	R6	Single
96130	HD 183899	-46±2 (F)	-45±5	R1	Single
98136	HD 188618	46±4 (F)	-15±5	R1	Binary? <sup>c</sup>
101328	HD 195455	19±7 (F), 10±6 (U)	10±6	R3	Single
105912	HD 204076	0±3 (F), 14±2 (U)	-17±7	R2	Binary
107027	HD 206144	122±5 (F), 121±2 (U)	117±8	R4	Single
109051	HD 209684	82±2 (U)	72±8	R4	Single
111563	HD 214080	16±2 (F)	12±4	R6	Single
112022	HD 214930	-60±4 (T)	-63±2	R3	Single
112482	HD 215733	-6±6 (T)	-15±2	R3	Single
113735	HD 217505	-17±1 (F)	-31±10	R2	Single
114690	HD 219188	73±19 (F), 98±19 (T)	64±3	R1	Single? <sup>d</sup>
115347	HD 220172	26±2 (F)	29±3	R6	Single
115729	HD 220787	26±2 (F)	26±3	R4	Single <sup>e</sup>
...	EC 05582-5816	85±13 (F)	81±10	R2	Single
...	EC 13139-1851	15±4 (F)	23±10	R2	Single
...	EC 20140-6935	-24±2 (U)	17±10	R2	Binary <sup>f</sup>
...	PB 5418	147±3 (U)	152±10	R2	Single
...	PHL 159	87±2 (U)	88±3	R2	Single

Note: <sup>a</sup> Spectrograph used for the observation: F=Feros, T=Tull and U=UVES

<sup>b</sup> References: R1=Gontcharov (2006), R2=Silva & Napiwotzki (2011), R3=Kharchenko et al. (2003), R4=Martin (2006), R5=Kordopartis et al. (2013), R6=Kilkenny & Hill (1975)

<sup>c</sup> Martin (2006) obtained the velocity 29±6 km s<sup>-1</sup> and quotes also -15 km s<sup>-1</sup> from Duffot et al. (1998).

<sup>d</sup> R2 gives the velocity as 84 km s<sup>-1</sup>

<sup>e</sup> R4 also gives velocities of 24.9±1.5 km s<sup>-1</sup> from Barbier-Brossat & Figon (2000) and 26.5±2.4 km s<sup>-1</sup> from Behr (2003).

<sup>f</sup> See text

spectroscopic binaries. HD 1999 and the double-lined eclipsing star HD 138503 (Martin 2003) are the only binary stars observed but not in Table 4. With present understanding of the formation of single and double runaway stars by the BSS and CES, it is not possible to interpret the low fraction of spectroscopic binaries as a pointer to the more important formation mechanism.

## 7. CONCLUDING REMARKS

Our sample of runaway stars is dominated by B stars which have been ejected from sites of recent star formation in the Galactic disk. Our non-LTE analysis of their C, N, Mg and Si abundances and published analyses of these elemental abun-

dances by the same non-LTE procedures in B stars in three open clusters in the Galactic disk show no abundance anomalies among the runaways that may be attributed to either of the leading two mechanisms (BSS and CES) capable obviously of producing runaways. The spread in abundances over a range of about 1 dex surely reflects the range in the Galactocentric distance of the birthplaces of the stars before they are ejected into the halo and the presence of an abundance gradient in the Galaxy. Consideration of either the projected rotational velocities or the radial velocities is presently unable to provide a determination of the relative probabilities of the BSS and CES in providing the runaway B stars. Yet, an intensive search for binaries among the B runaway population may yet shed light



on the relative contributions of the BSS and CES. Ability to identify runaway stars formed by the BSS will be enhanced by extending the non-LTE analysis to other elements, notably O and S which appear to have large excesses in  $[X/Fe]$  in the (few) LMXB secondaries analysed for this pair of elements.

We thank R. Napiwotzki, the referee, for constructive reports. DLL thanks A.B.S. Reddy for his help in preparing the manuscript for submission. CMM is grateful to the De-

partment of Education and Learning (DEL) in Northern Ireland and Queen's University Belfast for the award of a research studentship. This work was supported by the Science and Technology Faculty Council and the UIC. DLL thanks the Robert A. Welch Foundation of Houston, Texas for support through grant F-634. This work was partly funded by the Director General Discretionary fund at ESO. ESO programme IDs 091.D-0061(A) for FEROS and 093.D-0302(A) for UVES.

## REFERENCES

- Abt, H. A., Levato, H., & Grosso, M. 2002, *ApJ*, 573, 359  
 Abt, H. A., & Levy, S. G. 1978, *ApJS*, 36, 241  
 Aerts, C., De Cat, P., De Ridder, J., et al. 2006, *A&A*, 449, 305  
 Ballester, P., Modigliani, A., Boitquin, O., et al. 2000, *The Messenger*, 101, 31  
 Barbier-Brossat, M., & Figon, P. 2000, *A&AS*, 142, 217  
 Behr, B. B. 2003, *ApJS*, 149, 101  
 Blaauw, A. 1961, *Bull. Astron. Inst. Netherlands*, 15, 265  
 Blaauw, A. 1993, in *Astronomical Society of the Pacific Conference Series*, Vol. 35, *Massive Stars: Their Lives in the Interstellar Medium*, ed. J. P. Cassinelli & E. B. Churchwell, 207  
 Blaauw, A., & Morgan, W. W. 1954, *ApJ*, 119, 625  
 Brott, I., de Mink, S. E., Cantiello, M., et al. 2011, *A&A*, 530, A115  
 Brown, W. R. 2015, *ARA&A*, 53, 15  
 Daflon, S., & Cunha, K. 2004, *ApJ*, 617, 1115  
 Daflon, S., Cunha, K., de la Reza, R., Holtzman, J., & Chiappini, C. 2009, *AJ*, 138, 1577  
 de Bruijne, J. H. J., & Eilers, A.-C. 2012, *A&A*, 546, A61  
 de Zeeuw, T., Hoogerwerf, R., & de Bruijne, J. 2001, in *Astronomical Society of the Pacific Conference Series*, Vol. 228, *Dynamics of Star Clusters and the Milky Way*, ed. S. Deiters, B. Fuchs, A. Just, R. Spurzem, & R. Wielen, 201  
 Dekker, H., D'Odorico, S., Kaufer, A., Delabre, B., & Kotzlowski, H. 2000, in *Proc. SPIE*, Vol. 4008, *Optical and IR Telescope Instrumentation and Detectors*, ed. M. Iye & A. F. Moorwood, 534–545  
 Dufton, M., Figon, P., & Meyssonnier, N. 1998, *VizieR Online Data Catalog*, 3190  
 Dufton, P. L., Ryans, R. S. I., Trundle, C., et al. 2005, *A&A*, 434, 1125  
 Dunstall, P. R., Dufton, P. L., Sana, H., et al. 2015, *A&A*, 580, A93  
 Dyson, J. E., & Hartquist, T. W. 1983, *MNRAS*, 203, 1233  
 Fraser, M., Dufton, P. L., Hunter, I., & Ryans, R. S. I. 2010, *MNRAS*, 404, 1306  
 Garmany, C. D., Conti, P. S., & Massey, P. 1980, *ApJ*, 242, 1063  
 Gies, D. R., & Bolton, C. T. 1986, *ApJS*, 61, 419  
 Gontcharov, G. A. 2006, *Astronomy Letters*, 32, 759  
 González Hernández, J. I., Rebolo, R., & Israelian, G. 2008, *A&A*, 478, 203  
 Greenstein, J. L., & Sargent, A. I. 1974, *ApJS*, 28, 157  
 Guthrie, B. N. G. 1984, *MNRAS*, 210, 159  
 Gvaramadze, V. V., Gualandris, A., & Portegies Zwart, S. 2009, *MNRAS*, 396, 570  
 Heber, U., Edelmann, H., Napiwotzki, R., Altmann, M., & Scholz, R.-D. 2008, *A&A*, 483, L21  
 Hoffer, J. B. 1983, *AJ*, 88, 1420  
 Huang, Y., Liu, X.-W., Zhang, H.-W., et al. 2015, *Research in Astronomy and Astrophysics*, 15, 1240  
 Hubeny, I. 1988, *Computer Physics Communications*, 52, 103  
 Hubeny, I., Heap, S. R., & Lanz, T. 1998, in *Astronomical Society of the Pacific Conference Series*, Vol. 131, *Properties of Hot Luminous Stars*, ed. I. Howarth, 108–+  
 Hubeny, I., & Lanz, T. 1995, *ApJ*, 439, 875  
 Hunter, I., Dufton, P. L., Smartt, S. J., et al. 2007, *A&A*, 466, 277  
 Hunter, I., Brott, I., Lennon, D. J., et al. 2008, *ApJ*, 676, L29  
 Hunter, I., Brott, I., Langer, N., et al. 2009, *A&A*, 496, 841  
 Irrgang, A., Przybilla, N., Heber, U., Nieva, M. F., & Schuh, S. 2010, *ApJ*, 711, 138  
 Kaufer, A., Stahl, O., Tubbessing, S., et al. 1999, *The Messenger*, 95, 8  
 Keenan, F. P., Dufton, P. L., & McKeith, C. D. 1982, *MNRAS*, 200, 673  
 Kharchenko, N. V., Scholz, R.-D., Piskunov, A. E., Röser, S., & Schilbach, E. 2007, *Astronomische Nachrichten*, 328, 889  
 Kilkeny, D., & Hill, P. W. 1975, *MNRAS*, 172, 649  
 Kordopatis, G., Gilmore, G., Steinmetz, M., et al. 2013, *AJ*, 146, 134  
 Lanz, T., & Hubeny, I. 2007, *ApJS*, 169, 83  
 Leonard, P. J. T. 1989, *AJ*, 98, 217  
 Leonard, P. J. T. 1993, in *Astronomical Society of the Pacific Conference Series*, Vol. 45, *Luminous High-Latitude Stars*, ed. D. D. Sasselov, 360  
 Leonard, P. J. T., & Duncan, M. J. 1990, *AJ*, 99, 608  
 Leonard, P. J. T., & Fahlman, G. G. 1991, *AJ*, 102, 994  
 Luck, R. E., & Lambert, D. L. 2011, *AJ*, 142, 136  
 Lyubimkov, L. S., Lambert, D. L., Poklad, D. B., Rachkovskaya, T. M., & Rostopchin, S. I. 2013, *MNRAS*, 428, 3497  
 Lyubimkov, L. S., Rostopchin, S. I., Rachkovskaya, T. M., Poklad, D. B., & Lambert, D. L. 2005, *MNRAS*, 358, 193  
 Magee, H. R. M., Dufton, P. L., Keenan, F. P., et al. 1998, *A&A*, 338, 85  
 Martin, J. C. 2003, *PASP*, 115, 49  
 —. 2004, *AJ*, 128, 2474  
 —. 2006, *AJ*, 131, 3047  
 McDonald, I., Zijlstra, A. A., & Boyer, M. L. 2012, *MNRAS*, 427, 343  
 McEvoy, C. M., Dufton, P. L., Evans, C. J., et al. 2015, *A&A*, 575, A70  
 Mdzinarishvili, T. G., & Chargeishvili, K. B. 2005, *A&A*, 431, L1  
 Nieva, M. F., & Przybilla, N. 2006, *ApJ*, 639, L39  
 —. 2008, *A&A*, 481, 199  
 Nieva, M.-F., & Simón-Díaz, S. 2011, *A&A*, 532, A2  
 Philip, C. J., Evans, C. R., Leonard, P. J. T., & Frail, D. A. 1996, *AJ*, 111, 1220  
 Portegies Zwart, S. F. 2000, *ApJ*, 544, 437  
 Poveda, A., Ruiz, J., & Allen, C. 1967, *Boletín de los Observatorios Tonantzintla y Tacubaya*, 4, 86  
 Przybilla, N., Fernanda Nieva, M., Heber, U., & Butler, K. 2008, *ApJ*, 684, L103  
 Puls, J., Urbaneja, M. A., Venero, R., et al. 2005, *A&A*, 435, 669  
 Rolleston, W. R. J., Smartt, S. J., Dufton, P. L., & Ryans, R. S. I. 2000, *A&A*, 363, 537  
 Ryans, R. S. I., Dufton, P. L., Mooney, C. J., et al. 2003, *A&A*, 401, 1119  
 Sadakane, K., Arai, A., Aoki, W., et al. 2006, *PASJ*, 58, 595  
 Sana, H., de Koter, A., de Mink, S. E., et al. 2013, *A&A*, 550, A107  
 Santolaya-Rey, A. E., Puls, J., & Herrero, A. 1997, *A&A*, 323, 488  
 Sayer, R. W., Nice, D. J., & Kaspi, V. M. 1996, *ApJ*, 461, 357  
 Shaver, P. A., McGee, R. X., Newton, L. M., Danks, A. C., & Pottasch, S. R. 1983, *MNRAS*, 204, 53  
 Silva, M. D. V., & Napiwotzki, R. 2011, *MNRAS*, 411, 2596  
 Simón-Díaz, S., Herrero, A., Uytterhoeven, K., et al. 2010, *ApJ*, 720, L174  
 Smartt, S. J., Dufton, P. L., & Lennon, D. J. 1997, *A&A*, 326, 763  
 Tetzlaff, N., Neuhäuser, R., & Hohle, M. M. 2011, *MNRAS*, 410, 190  
 Tobin, W. 1987, in *IAU Colloq. 95: Second Conference on Faint Blue Stars*, ed. A. G. D. Philip, D. S. Hayes, & J. W. Liebert, 149–158  
 Trundle, C., Dufton, P. L., Hunter, I., et al. 2007, *A&A*, 471, 625  
 Tull, R. G., MacQueen, P. J., Sneden, C., & Lambert, D. L. 1995, *PASP*, 107, 251  
 Wolff, S. C., Edwards, S., & Preston, G. W. 1982, *ApJ*, 252, 322  
 Zwicky, F. 1957, *Morphological astronomy*